IEEE Photonics Journal
An IEEE Photonics Society Publication

Open Access

Experimental Demonstration of 1.2-Tb/s Optical PDM SCFDM Superchannel Multicasting by HNLF

Volume 5, Number 5, October 2013

Yuanxiang Chen
Juhao Li, Member, IEEE
Paikun Zhu
Yingying Xu
Yongqi He
Zhangyuan Chen, Member, IEEE

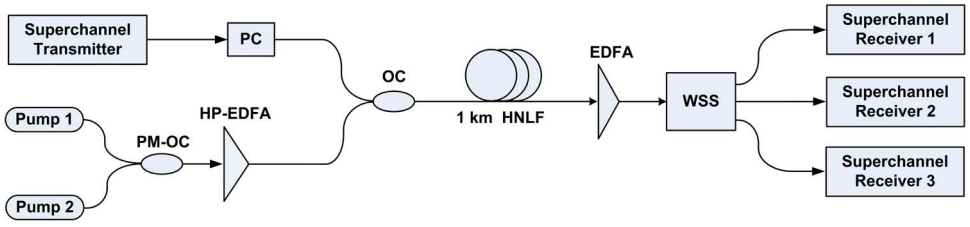

DOI: 10.1109/JPHOT.2013.2280534
1943-0655 © 2013 IEEE

IEEE photonics SOCIETY

IEEE

Experimental Demonstration of 1.2-Tb/s Optical PDM SCFDM Superchannel Multicasting by HNLF

Yuanxiang Chen, Juhao Li, *Member, IEEE*, Paikun Zhu, Yingying Xu, Yongqi He, and Zhangyuan Chen, *Member, IEEE*

State Key Laboratory of Advanced Optical Communication Systems and Networks, Peking University, Beijing, China

DOI: 10.1109/JPHOT.2013.2280534

Manuscript received August 4, 2013; revised August 25, 2013; accepted August 28, 2013. Date of publication September 4, 2013; date of current version September 10, 2013. This work was supported by the National Basic Research Program of China (973 Program) under Grants 2010CB328201 and 2010CB328202; by the National Natural Science Foundation of China (NSFC) under Grants 60907030, 61275071, 60736003, and 60931160439; and by the National Hi-Tech Research and Development Program of China under Grant 2011AA01A106. Corresponding author: J. Li (e-mail: juhao_li@pku.edu.cn).

Abstract: Threefold 1.2-Tb/s optical polarization-division-multiplexing (PDM) single-carrier frequency-division-multiplexing (SCFDM) and orthogonal-frequency-division-multiplexing (OFDM) superchannel multicasting, utilizing multiple-pump four-wave mixing (FWM) by highly nonlinear fiber (HNLF), is proposed and experimentally demonstrated in this paper. The optical signal noise ratio (OSNR) penalties of the newly generated SCFDM and OFDM superchannels, at the bit error rate (BER) of 10^{-3}, are 2.6 dB and 3.1 dB, respectively. Optimal pump power and signal power are also investigated for the two superchannels. The two superchannels have similar optimal pump power, whereas the SCFDM superchannel has higher optimal signal power due to the lower peak-to-average power ratio (PAPR).

Index Terms: Superchannel multicasting, four-wave-mixing (FWM), orthogonal-frequency-division-multiplexing (OFDM), single-carrier frequency-division-multiplexing (SCFDM).

1. Introduction

In recent years, with the increasing bandwidth requirement of future optical networks, optical superchannel has gained great interest for its high spectral efficiency (SE) to transfer large volume data [1]–[3]. The single-carrier frequency-division-multiplexing (SCFDM) utilizing discrete Fourier transform (DFT) spread orthogonal-frequency-division-multiplexing (OFDM), which has high tolerance against chromatic dispersion (CD) and polarization mode dispersion (PMD), is emerging as one of the most promising technology for optical superchannel [4]–[6]. Compared with OFDM, the SCFDM has similar tolerance to linear dispersion impairments and overall complexity, while achieves better tolerances to nonlinear transmission impairments because of lower peak-to-average power ratio (PAPR) [7]–[9].

Wavelength multicasting is expected to be a key technique to realize data point-to-multipoint connections in wavelength-division-multiplexing (WDM) systems [10]–[12]. It can effectively improve the network efficiency and increase the network throughput. Similar to wavelength multicasting, optical superchannel multicasting can also enhance network performance by generating many superchannel copies. Compared with wavelength multicasting with fixed signal bit rate and modulation format, optical superchannel multicasting should be transparent to the signal format and should support multi-band polarization-division-multiplexing (PDM) signals. In our previous work

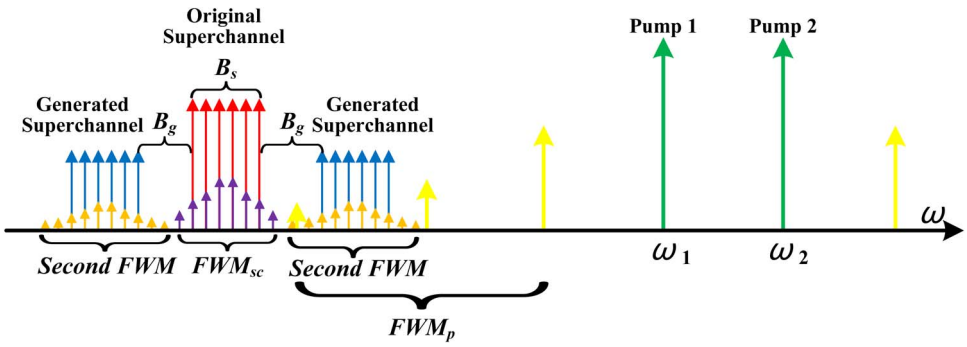

Fig. 1. Operation principle of 3-fold optical superchannel multicasting.

[13] and [14], 400 Gb/s optical PDM OFDM superchannel multicasting by multiple-pump four-wave-mixing (FWM) and 240 Gb/s optical PDM–OFDM superchannel conversion based on pump-switching FWM scheme in highly nonlinear fiber (HNLF) were experimentally demonstrated, respectively. In this paper, we extend the superchannel data rate to 1.2 Tb/s and experimentally demonstrate threefold 1.2 Tb/s optical PDM SCFDM and OFDM superchannel multicasting. What is more, we analyze the impact of different PAPR characteristics in the process of multicasting for the two superchannels. Multicasting performance comparison and signal and pump power optimization are also performed for the two superchannels. The results show that compared with OFDM superchannel, the SCFDM superchannel suffers lower OSNR penalty due to the lower PAPR in the process of FWM. The two superchannels have same optimal pump power while SCFDM superchannel has higher optimal signal power.

2. Technique Principle

We utilize co-polarized multiple-pump FWM scheme to realize the multicasting of PDM optical superchannel. In multiple-pump FWM scheme, the signal can be placed in the middle of the two pumps [15], [16]. However, this scheme is polarization sensitive and it does not apply to PDM signal multicasting. So we only consider the scheme that the signal spectrally located at the one side of the pumps. As shown in Fig. 1, for threefold optical superchannel multicasting, two co-polarized pumps are needed. PDM SCFDM/OFDM superchannel (red in Fig. 1) with center frequency of ω_s and two co-polarized pumps (pump 1 and pump 2) with frequency of ω_1, ω_2 $(\omega_s < \omega_1 < \omega_2)$ are coupled into the HNLF. After FWM process, two superchannel copies with center frequency of ω_{c1} and ω_{c2} (blue in Fig. 1) are generated at the both sides of the original superchannel. The frequency relationships of the two pumps, the original superchannel, and the two generated superchannels are listed below:

$$\omega_2 - \omega_1 = B_s + B_g \tag{1}$$

$$\omega_{C1} = \omega_s - \omega_2 + \omega_1 \tag{2}$$

$$\omega_{C2} = \omega_s - \omega_1 + \omega_2 \tag{3}$$

where B_s represents the bandwidth of the superchannel and B_g represents the guard bandwidth between the two adjacent superchannels.

Then we analyze the nonlinear impairments of the multicasting. Besides the newly generated superchannels, the numerous subcarriers in an SCFDM/OFDM superchannel will also produce other FWM products as they propagate through the HNLF. Here, we only consider the FWM products that are spectrally located at the original superchannel and the generated superchannels. The most significant FWM products are generated by the degenerate FWM of the pumps (yellow in Fig. 1, FWM_p) and the mixing between the subcarriers themselves (purple in Fig. 1, FWM_{sc}). In our multicasting scheme, we preserve sufficiently wide guard band to avoid interference from FWM_p and FWM_{sc} to the newly generated superchannels. The guard bandwidth can prevent the newly

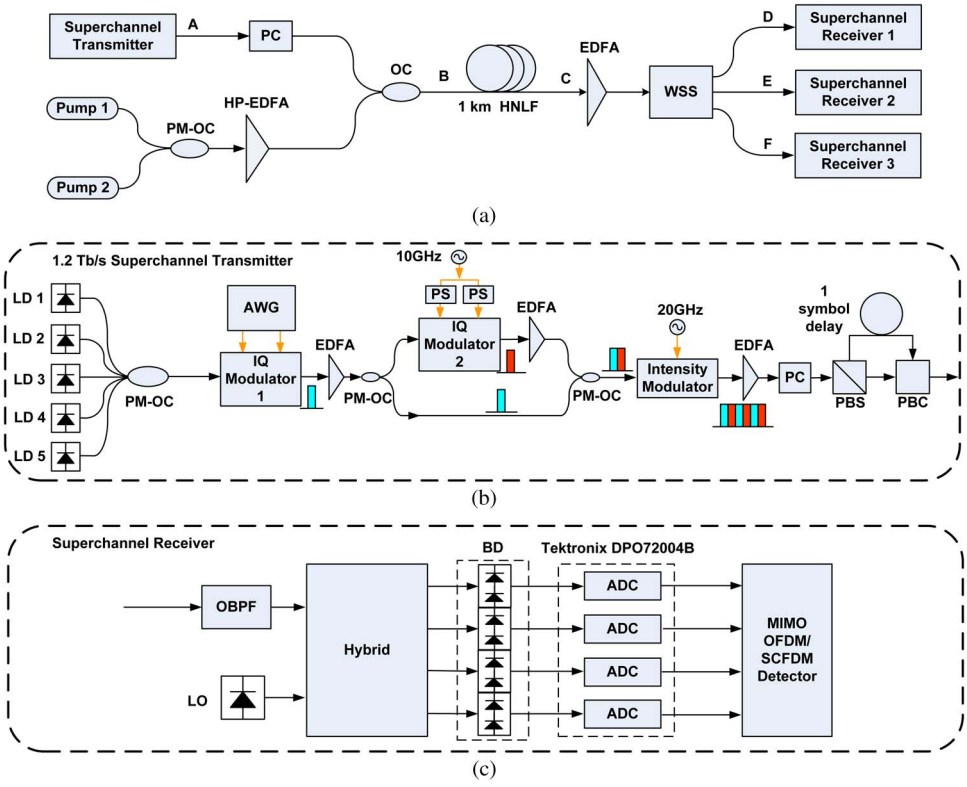

Fig. 2. Experiment setup of (a) 1.2 Tb/s SCFDM/OFDM superchannel multicasting, (b) superchannel transmitter, and (c) superchannel receiver.

generated superchannel from falling on FWM_p and FWM_{sc}. However, FWM_{sc} will interact with the pumps to produce secondary FWM products along the HNLF. The secondary FWM products will fall on the newly generated superchannels, and they will degrade the multicasting performance. The secondary FWM products are shown in orange in Fig. 1. From above analysis, we know both the original superchannel and the new generated superchannel will suffer nonlinear impairments after multicasting. The impairments are relative with the parameters of the HNLF, signal power, pump power, and signal form.

3. Experiment Setup

Fig. 2(a) shows the experimental setup to verify threefold Tb/s optical PDM SCFDM/OFDM superchannel multicasting. On the signal branch, we adopt the similar scheme that was shown in our previous work [6] to construct the Tb/s SCFDM/OFDM superchannel. The center frequency of the superchannel is 192.340 THz (1559.68 nm). The superchannel consists of 30 subbands, each of which is PDM-quadrature-phase-shift-keying (QPSK) modulated. The bandwidth of the superchannel is 300 GHz, and the total data rate is 1.2 Tb/s. On the pump branch, two pumps (pumps 1 and 2) with center frequencies of 193.150 THz (1553.20 nm) and 193.475 THz (1550.61 nm) are coupled by a polarization maintaining optical coupler (PM-OC) as co-polarized pumps. A guard band of 25 GHz is preserved for the FWM idlers generated by the pumps. To achieve balanced conversion efficiency for both polarizations of the multicasted superchannels, we use a polarization controller (PC) to adjust the polarization state of the superchannels. After being amplified by a high-power erbium-doped fiber amplifier (HP-EDFA), the pumps are coupled with the superchannel by an optical coupler (OC) and sent into the HNLF for multicasting. To reduce the phase mismatch and improve conversion efficiency over wide frequency band, we select HNLF with low dispersion slope and high nonlinear coefficient. In our experiment, the HNLF has a length of 1 km, a nonlinear

coefficient of 10 W^{-1}/km, an attenuation coefficient of 0.939 dB/km, a zero-dispersion wavelength of 1567 nm, and a dispersion slope of 0.03 ps/nm^2/km. After FWM in HNLF, two phase non-conjugate copies (S1 and S3) of the original superchannel (S2) are generated at the output of the HNLF. After amplification, a wavelength select switch (WSS) with bandwidth of 310 GHz selects the superchannels to receiver for coherent detection.

We adopt the similar scheme in [6] to generate and receive the baseband SCFDM/OFDM signal. For OFDM signal, the mapped QPSK signals are grouped into blocks with 200 OFDM symbols. For each OFDM symbol, 108 subcarriers are used for data transmission, 16 subcarriers as guard band, and four subcarriers as pilots. A 128-point inverse DFT (IDFT) transforms the subcarriers to a complex time domain signal. Before the signal is transmitted, both cyclic prefix (CP) and cyclic suffix (CS) with a length of eight subcarriers are inserted. Preamble is added to each block. The preamble includes two Chu-sequences of 64-subcarrier length for synchronization and four Chu-sequences of 128-subcarrier length for channel estimation. At the receiver, the signal is equalized in frequency domain after synchronization. For SCFDM signal, additional M-point DFT operation and subcarrier mapping at the transmitter and M-point IDFT at the receiver are performed. For OFDM signal, each point in time domain is the sum of all subcarriers, and cophased adding and subtracting will result in significant power difference. Compared with OFDM, the original signal of SCFDM is pulse-shaped QPSK signal with low PAPR. The subcarrier-mapping is interpolation and filtering for original QAM signal. So the PAPR of the SCFDM is lower than that of the OFDM.

The detailed setup of SCFDM/OFDM superchannel transmitter is depicted in Fig. 2(b). We use five lasers (LD1 to LD5) with line-width of 5 kHz to generate the 1.2 Tb/s PDM-SCFDM/OFDM superchannel. The frequency spacing of the adjacent lasers for the five lasers is 60 GHz. The corresponding center wavelength of the LD1, LD2, LD3, LD4, and LD5 are 1558.72 nm, 1559.20 nm, 1559.68 nm, 1560.16 nm, and 1560.64 nm, respectively. After being combined by PM-OC, the five lasers are sent to the IQ Modulator 1 for modulation. A Tektronix arbitrary waveform generator (AWG7122B) operating at 10 GS/s is used to generate offline-calculated baseband SCFDM/OFDM signals. The in-phase (I) and quadrature (Q) parts of the signals are directly converted to five optical carriers by an optical IQ MZM. Five odd subbands are obtained after the IQ modulator 1. Then we adopt the same scheme in [17] to generate the even subbands. The odd subbands are split into two streams by 1 $\times$ 2 PM-OC after an EDFA. The odd subband is split into two streams by 1 $\times$ 2 PM-OC. The lower stream passes directly without any change while the upper one passes a frequency shifter, which is realized by driving the IQ modulator 2 with 10 GHz radio frequency (RF) signal. Two phase shifters (PS) are used for adjusting the phase difference between the two arms. Before being combined by 2 $\times$ 1 PM-OC, the even and odd subbands are delayed by optical patchcords with different length for decorrelation. Then the two subbands pass the three-tone generator, which is realized by driving the intensity modulator with 20 GHz RF. Thus the 30-subband superchannel is generated with a frequency spacing of 10 GHz. The PDM is emulated with a PC, a polarization beam splitter (PBS), a tunable optical delay line, and a polarization beam combiner (PBC). The delay of the optical delay line is exactly one SCFDM/OFDM symbol. At the output of the transmitter, a superchannel with total data rate of 1.2 Tb/s is generated. The superchannel consists of continuous 30 subbands, each of which is PDM-QPSK modulated.

The detailed setup of SCFDM/OFDM superchannel receiver is depicted in Fig. 2(c). At the receiver, the received signal is sent into a 90° hybrid with a local oscillator (LO) and interferes with each other before being detected by four balanced detectors (BD). Then the polarization diverse signals are sampled at 50 GS/s by a real-time digital storage oscilloscope (Tektronix DPO72004B). The sampled data are processed offline. The optical band-pass filter (OBPF) at the receiver has a bandwidth of 60-GHz. The LO is a tunable laser with the line-width of 100 kHz.

4. Experimental Results

Fig. 3(a)–(c) shows the optical spectra of 1.2 Tb/s PDM SCFDM/OFDM superchannel, input of the HNLF, and output of the HNLF, respectively. The output of the HNLF consists of three super-channels and other FWM idlers. The FWM idlers generated by the pumps are accurately located in

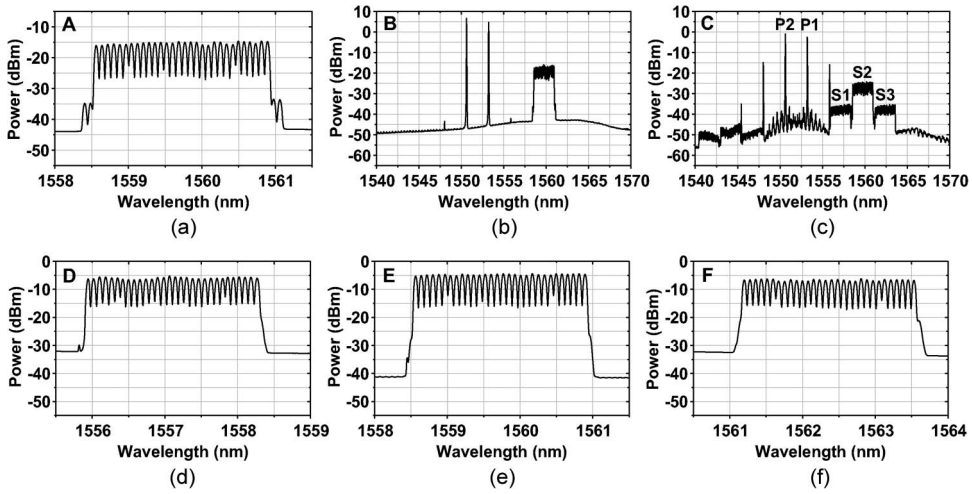

Fig. 3. Optical spectra for (a) 1.2 Tb/s superchannel, (b) input of the HNLF, (c) output of the HNLF, and (d)–(f) three superchannels after the WSS.

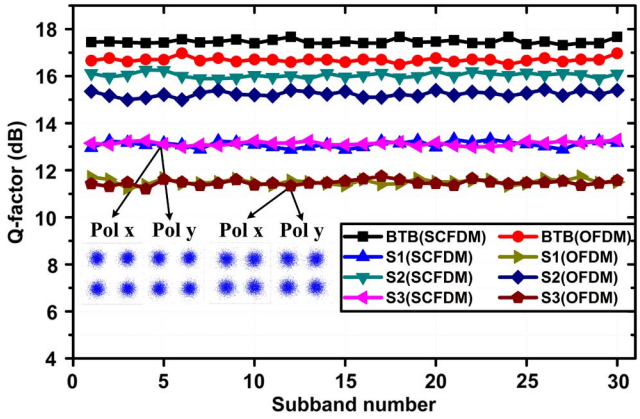

Fig. 4. Q-factor performance of all the subbands.

the guard band between the adjacent superchannnels, and they can be filtered out by the WSS. The optical signal noise ratio (OSNR) of the two newly generated superchannels is 17.5 dB. The conversion efficiency is −20 dB. The three superchannels after the WSS are shown in Fig. 3(d)–(f), respectively.

Fig. 4 shows the Q-factor performance of the multicasted superchannels. To evaluate the performance of the multicasting functionality, the back-to-back (BTB) Q-factors of all 30 SCFDM/OFDM subbands are measured as reference. After multicasting, we can see the subbands have similar performance in each superchannel. The two newly generated SCFDM superchannnels suffers a Q-factor penalty of 4.5 dB, while the OFDM superchannel suffers a Q-factor penalty of 5 dB. Fig. 5 shows the bit-error-rate (BER) performance. We measure the tenth subband of each superchannel as reference. It is observed that, at FEC BER limit of 10^{-3}, the OSNR penalties of the original SCFDM and OFDM superchannels are 0.7 dB and 1 dB, respectively. The newly generated SCFDM superchannel suffers an OSNR penalty of 2.6 dB, while the OFDM superchannel suffers an OSNR penalty of 3.1 dB. In our experimental setup for Q-factor and OSNR penalty test, the input signal power and input pump power for the two superchannels are identical. The input signal power is 9 dBm, and the total input pump power is 21 dBm. After multicasting, the converted superchannels have the same power level for the two superchannels. The EDFA configurations for

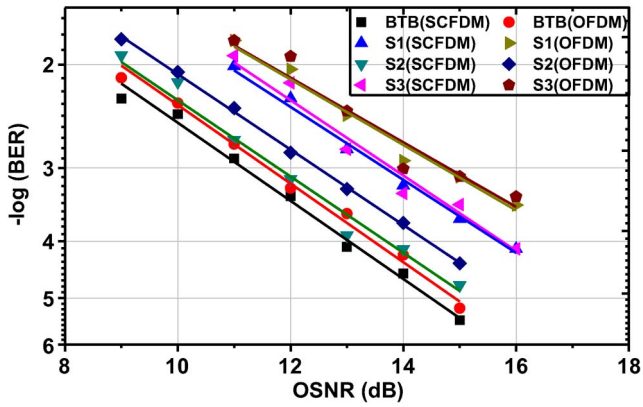

Fig. 5. BER performance versus OSNR.

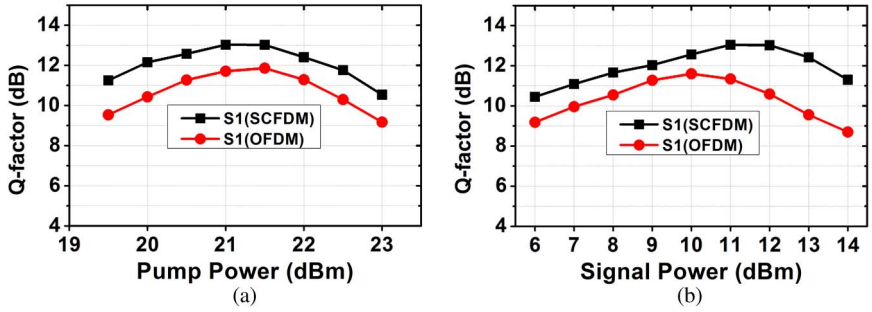

Fig. 6. Q-factor performance versus input (a) pump power and (b) signal power.

the two superchannels are also the same. The different multicasting performance is due to different PAPR characteristics of the two superchannels. The OFDM superchannel with higher PAPR also suffers from higher in-band nonlinear impairment and corresponding higher influence of secondary FWM products.

We also investigate multicasting performance optimization by adjusting the pump power and signal power. We measure the Q-factor performance of the tenth subband in the SCFDM/OFDM superchannel 1 (S1). In Fig. 6(a), the pump power increases from 19.5 dBm to 23 dBm, while the signal power is fixed at 10 dBm. From the results, we can see that OFDM superchannel and SCFDM superchannel have the same optimal input pump power of 21.5 dBm. The lower pump power will degrade the Q-factor performance due to the lower OSNR, while the higher pump power will intensify the stimulated Brillouin scattering (SBS) effects which also will degrade the Q-factor performance. When the pump power reaches the SBS threshold, SBS will deplete the effective pump power and it will degrade the conversion efficiency. When the pump power is much higher than the SBS threshold, part of the power will be fed to the forward direction again due to the second order SBS process [18], [19]. The second order wave moves in the same direction as the original signal direction, and it will worsen the multicasting performance. In our experiment, we observe obvious power dithering of the multicasted signal when the pump power is higher than 22 dBm. The multicasting performance degrades when the pump power is higher than SBS threshold. Phase modulation of the pump can suppress the SBS but will also distort the phase of the multicasted signal. In this case, an advanced phase modulation scheme might be necessary. In Fig. 6(b), the pump power is fixed at 21 dBm, while the signal power increases from 6 dBm to 14 dBm. We can see that both the SCFDM superchannel and OFDM superchannel have an optimal input signal power. It is because that the lower signal power will reduce the OSNR of the multicasting superchannel, while

the higher signal power causes strong crosstalk, and they both degrade the Q-factor performance. The optimal input signal power of SCFDM superchannel is 1.5 dBm higher than that of OFDM due to the lower PAPR.

5. Conclusion

In this paper, threefold 1.2 Tb/s optical PDM SCFDM and OFDM superchannel multicasting by HNLF is experimentally demonstrated and compared. The OSNR penalties of the newly generated SCFDM and OFDM superchannels at the BER of 10^{-3} are 2.6 dB and 3.1 dB, respectively. Optimal pump power and signal power are also investigated for the two superchannels. Compared with OFDM, SCFDM superchannel has similar optimal pump power while has higher optimal signal power due to the lower PAPR.

References

[1] X. Liu and S. Chandrasekhar, "Beyond 1-Tb/s superchannel transmission," presented at the IEEE Photon. Conf. Inst. Elect. Electron. Eng., Arlington, VA, USA, 2011, Paper ThBB1.
[2] J. Yu, Z. Dong, X. Xiao, Y. Xia, S. Shi, C. Ge, W. Zhou, N. Chi, and Y. Shao, "Generation, transmission and coherent detection of 11.2 Tb/s (112x100Gb/s) single source optical OFDM superchannel," presented at the Opt. Fiber Commun. Conf., Los Angeles, CA, USA, Mar. 2011, Paper PDPA6.
[3] E. Torrengo, R. Cigliutti, G. Bosco, G. Gavioli, A. Alaimo, A. Arena, V. Curri, F. Forghieri, S. Piciaccia, M. Belmonte, A. Brinciotti, A. L. Porta, S. Abrate, and P. Poggiolini, "Transoceanic PM-QPSK Terabit superchannel transmission experiments at Baud-rate subcarrier spacing," presented at the Eur. Conf. Opt. Commun., Torino, Italy, 2010, Paper We.7.C.2.
[4] Q. Yang, Z. He, Z. Yang, S. Yu, X. Yi, and W. Shieh, "Coherent optical DFT-spread OFDM transmission using orthogonal band multiplexing," *Opt. Exp.*, vol. 20, no. 3, pp. 2379–2385, 2012.
[5] J. Li, S. Zhang, F. Zhang, and Z. Chen, "A novel coherent optical single-carrier frequency-division-multiplexing (CO-SCFDM) scheme for optical fiber transmission systems," presented at the Photon. Switching, Montery, CA, USA, 2010, JTuB41.
[6] C. Zhao, Y. Chen, S. Zhang, J. Li, F. Zhang, L. Zhu, and Z. Chen, "Experimental demonstration of 1.08 Tb/s PDM CO-SCFDM transmission over 3170 km SSMF," *Opt. Exp.*, vol. 20, no. 2, pp. 787–793, Jan. 16, 2012.
[7] F. Zhang, C. Yang, X. Fang, T. Zhang, and Z. Chen, "Nonlinear performance of multi-granularity orthogonal transmission systems with frequency division multiplexing," *Opt. Exp.*, vol. 21, no. 5, pp. 6115–6130, Mar. 11, 2013.
[8] S. L. Jansen, I. Morita, K. Forozesh, S. Randel, D. van den Bornel, and H. Tanaka, "Optical OFDM, a hype or is it for real?" presented at the Eur. Conf. Opt. Commun., Brussels, Belgium, Sep. 2008, Paper Mo.3.E.3.
[9] G. Berardinelli, L. A. Ruiz De Temino, S. Frattasi, M. Rahman, and P. Mogensen, "OFDMA vs. SC-FDMA: Performance comparison in local area IMT-A scenarios," *IEEE Wireless Commun.*, vol. 15, no. 5, pp. 64–72, Oct. 2008.
[10] X. Zhang, J. Wei, and C. Qiao, "On fundamental issues in IP over WDM multicast," in *Proc. Int. Conf. Comput., Commun. Netw.*, Boston, MA, USA, 1999, pp. 84–90.
[11] C. Y. Li, P. K. A. Wai, X. C. Yuan, and V. O. K. Li, "Multicasting in deflection-routed all-optical packet-switched networks," in *Proc. IEEE Global Telecommun. Conf.*, Taipei, Taiwan, 2002, pp. 2842–2846.
[12] R. K. Pankaj, "Wavelength requirements for multicasting in all-optical networks," *IEEE/ACM Trans. Netw.*, vol. 7, no. 3, pp. 414–424, Jun. 1999.
[13] Y. Chen, J. Li, P. Zhu, B. Guo, L. Zhu, Y. He, and Z. Chen, "Experimental demonstration of 400 Gb/s optical PDM-OFDM superchannel multicasting by multiple-pump FWM in HNLF," *Opt. Exp.*, vol. 21, no. 8, pp. 9915–9922, 2013.
[14] Y. Chen, J. Li, P. Zhu, Y. Xu, Y. Zhong, B. Guo, Y. He, and Z. Chen, "A novel pump-switching FWM scheme for optical superchannel conversion in EON," *IEEE Photon. Technol. Lett.*, vol. 25, no. 16, pp. 1634–1637, Aug. 2013.
[15] A. Wiberg, E. Myslivets, C. Brès, and S. Radic, "Low distortion 6-copy multicasting of analog signal using self-seeded parametric mixer," presented at the Eur. Conf. Opt. Commun., Geneva, Switzerland, Sep. 2011, Paper Th.12.LeCervin.6.
[16] C. Brès, A. Wiberg, B. Kuo, E. Myslivets, and S. Radic, "320 Gb/s RZ-DPSK data multicasting in self seeded parametric mixer," presented at the Opt. Fiber Commun. Conf., Los Angeles, CA, USA, Mar. 2011, Paper OThC7.
[17] X. Liu, S. Chandrasekhar, and B. Zhu, "Transmission of a 448-Gb/s reduced-guard-interval CO-OFDM signal with a 60-GHz optical bandwidth over 2000 km of ULAF and five 80-GHz-grid ROADMs," presented at the Opt. Fiber Commun. Conf., San Diego, CA, USA, 2010, Paper PDPC2.
[18] M. F. Ferreira, "Limitations imposed by stimulated Brillouin scattering on uni- and bi-directional transmission systems using active fibres," *Electron. Lett.*, vol. 31, no. 14, pp. 1182–1183, Jul. 1995.
[19] L. Chen and X. Bao, "Analytical and numerical solutions for steady state stimulated Brillouin scattering in a single-mode fiber," *Opt. Commun.*, vol. 152, no. 1-3, pp. 65–70, Jun. 1998.